

## **Best Paper Award**

The following paper "Creep Deformation Anisotropy in Single Crystal Superalloys," by P. Caron, Y. Ohta, Y.G. Nakagawa and T. Khan was selected by the Honors and Awards Subcommittee of the Seven Springs International Symposium Committee as the Best Paper of the Sixth Symposium. The criteria for judging all papers was based on technical excellence, originality, and pertinence to the superalloy and gas turbine industries.

## CREEP DEFORMATION ANISOTROPY

### IN SINGLE CRYSTAL SUPERALLOYS

P. Caron\*, Y. Ohta\*\*, Y.G. Nakagawa\*\* and T. Khan\*

\* Office National d'Etudes et de Recherches Aéronautiques (ONERA)  
B.P. 72, 92322 Châtillon Cedex, France

\*\* IHI Research Institute  
Toyosu, Koto-ku, Tokyo 135, Japan

#### Abstract

The anisotropic behaviour in creep of a number of single crystal superalloys (CMSX-2, alloy 454, MXON and CMSX-4) was investigated in the temperature range 760–1050°C as a function of the  $\gamma'$  particle size. The particle size is shown to have a spectacular effect both on the creep behaviour and stress rupture life at intermediate temperatures (760–850°C). In this temperature range, a  $\gamma'$  particle size of about 0.5  $\mu\text{m}$  which results in optimum creep strength for the [001] orientation drastically reduces the stress rupture life for the  $[\bar{1}11]$  orientation. However, a very fine  $\gamma'$  particle size ( $\approx 0.2 \mu\text{m}$ ) leads to a dramatic improvement for the  $[\bar{1}11]$  orientation, which becomes the strongest. In the CMSX-2 alloy, for instance, the creep anisotropy between [001] and  $[\bar{1}11]$  can be totally eliminated for a  $\gamma'$  particle size of about 0.3  $\mu\text{m}$ . The relationship between the creep behaviour of various single crystals and their deformation microstructures was analyzed in detail. At higher temperatures (950–1050°C) the effect of orientation and the particle size on creep strength is considerably reduced.

## Introduction

Single crystal alloys for blade applications have now become an industrial reality. Because of their highly anisotropic properties, these materials pose unique challenges for use as structural materials. The orientation of single crystal blades is [001], which provides the best combination of properties that are required in the hot section of an aircraft turbine. Although the blade is essentially subjected to centrifugal loading along the [001] axis, some multiaxial stresses are generated locally due to the complex shape of the blade root and, in some cases, because of the presence of intricate cooling schemes in the airfoil section. Moreover, temperature gradients between different parts of the blade cause high thermal stresses along various directions. An important requirement for a proper and efficient design of single crystal blades is the development of appropriate constitutive models. Extensive work is being carried out both in Europe and USA to develop such models. The micro-mechanical approach for modelling requires in particular that the complex anisotropy of plastic deformation be fully identified and characterized. One of the major objectives of this paper is to perform a detailed study of the creep deformation anisotropy of various single crystal superalloys in the temperature range 760-1050°C as a function of precipitation heat treatments. A detailed investigation was carried out on the CMSX-2 alloy, but some results were also obtained on other alloys (CMSX-4, alloy 454, MXON) in order to propose a coherent explanation regarding the anisotropic creep behaviour of the single crystal superalloys.

## Experimental procedures

The compositions of the different studied alloys are presented in the Table I. The CMSX-2 and CMSX-4 alloys were developed by Cannon-Muskegon Corporation (1,2) whereas alloy 454 was developed by United Technologies (3). The CMSX-4 alloy was chosen, since it contains rhenium, an element not commonly used in superalloys. The MXON experimental alloy was developed by ONERA (4). Dendritic single crystal rods or plates were grown by the withdrawal process using a seed or a selector. The crystallographic orientations of the single crystals were checked by the Laue X-ray back reflection technique. In the case of CMSX-2 and alloy 454, the selected crystal orientations fully covered the stereographic triangle. For the other alloys, the single crystals were grown only in the [001] and  $[\bar{1}11]$  orientations.

Table I. Chemical compositions (wt.%) of the single crystal alloys

Alloy	Ni	Co	Cr	W	Mo	Re	Al	Ti	Ta
CMSX-2	Base	5	8	8	0.6	-	5.5	1	6
CMSX-4*	Base	9.2	6.6	5.9	0.6	3.3	5.6	0.9	6.2
MXON	Base	5	8	8	2	-	6.1	-	6
Alloy 454	Base	5	10	4	-	-	5	1.5	12

\* Chemical analysis at IHI

All single crystals were first heat treated at temperatures around 1300°C, followed by air quenching, in order to solutionize the  $\gamma/\gamma'$  eutectic pools and to partially homogenize the dendritic segregation. The CMSX-4 single crystals were subjected to a two-step solutioning heat treatment recommended by Cannon-Muskegon to reduce the volume fraction of residual  $\gamma/\gamma'$  eutectic pools. These single crystals were then subjected to different precipitation heat treatments resulting in various  $\gamma'$  particle mean sizes, ranging from 0.2 to 0.54  $\mu\text{m}$ .

Constant load stress-rupture tests were performed in air in the

temperature range 760-1050°C. Some creep tests were interrupted before rupture in order to prepare samples for transmission electron microscopy (TEM) examinations. Thin foils were prepared by twin-jet electropolishing using a solution of 45% butylcellosolve, 45% acetic acid and 10% perchloric acid at 0°C and 25 V. These foils were examined both at IHI and ONERA.

### Experimental results

#### Creep properties at intermediate temperatures (760-850°C)

Previous work has shown that the creep behaviour of single crystal superalloys is strongly dependent on the orientation at intermediate temperatures (5-8). Another study by Caron and Khan (9) on the CMSX-2 alloy had demonstrated that the creep behaviour of [001] oriented single crystal could be modified by varying the size (and perhaps the morphology) of the strengthening  $\gamma'$  precipitates. It was therefore decided to undertake a detailed investigation on the effect of heat treatments on the creep behaviour of selected Ni-based single crystal alloys in various orientations.

Three different precipitation heat treatments were applied to the CMSX-2 single crystals in order to produce  $\gamma'$  sizes of 0.23, 0.3 and 0.45  $\mu\text{m}$  respectively. Stress rupture lives as a function of orientation and heat treatments are shown in the stereographic triangles of Figure 1. The creep behaviour at 760°C for the three principal orientations [001],  $[\bar{1}11]$  and [011] is illustrated by the typical creep curves of Figure 2.

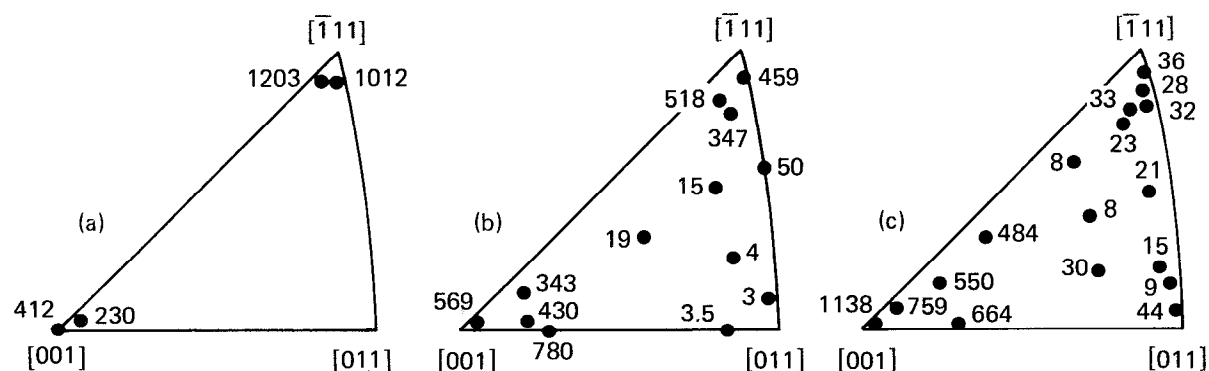


Figure 1 — Orientation dependence of the stress rupture life (in hours) at 760°C and 750 MPa of CMSX-2 single crystals, as a function of  $\gamma'$  precipitate size : (a) 0.23  $\mu\text{m}$ , (b) 0.3  $\mu\text{m}$  and (c) 0.45  $\mu\text{m}$ .

In the [001] orientation, the longest creep lives are obtained with the largest precipitates (0.45  $\mu\text{m}$ ). We have previously shown that if the precipitate size is much larger than 0.5  $\mu\text{m}$  the stress rupture lives are again substantially lowered at intermediate temperatures (10). A reduction of the precipitate size increases both the amplitude of the primary creep and the secondary creep rate, thereby resulting in a poor stress rupture life. On the other hand, the  $[\bar{1}11]$  oriented crystals containing  $\gamma'$  precipitates of 0.45  $\mu\text{m}$  exhibit extremely poor creep strengths and large elongations to rupture due to an almost total absence of strain hardening.

Contrary to the case of [001] specimens, decreasing the  $\gamma'$  size led to a spectacular increase of the creep strength of the  $[\bar{1}11]$  crystals: a particle size of 0.23  $\mu\text{m}$ , the smallest achieved in this investigation, led to a 30-fold increase in the stress rupture life at 760°C compared with that obtained with a particle size of 0.45  $\mu\text{m}$ . The  $[\bar{1}11]$  single crystals containing the smallest particles exhibited very low creep rates and the rupture occurred after a small elongation. The single crystals oriented far away from the [001] and  $[\bar{1}11]$  exhibit short rupture lives, irrespective of the precipitation heat treatments, but the effect is much more drastic near the  $[\bar{1}11]$  orientation than near the [001] orientation. The creep behaviour is

however dependent on the  $\gamma'$  size in the case of [011] oriented crystals: specimens containing 0.3  $\mu\text{m}$  particles do not exhibit any strain hardening and the rupture occurs rapidly after large elongations, whereas those having the largest particles showed some strain hardening and lower elongations.

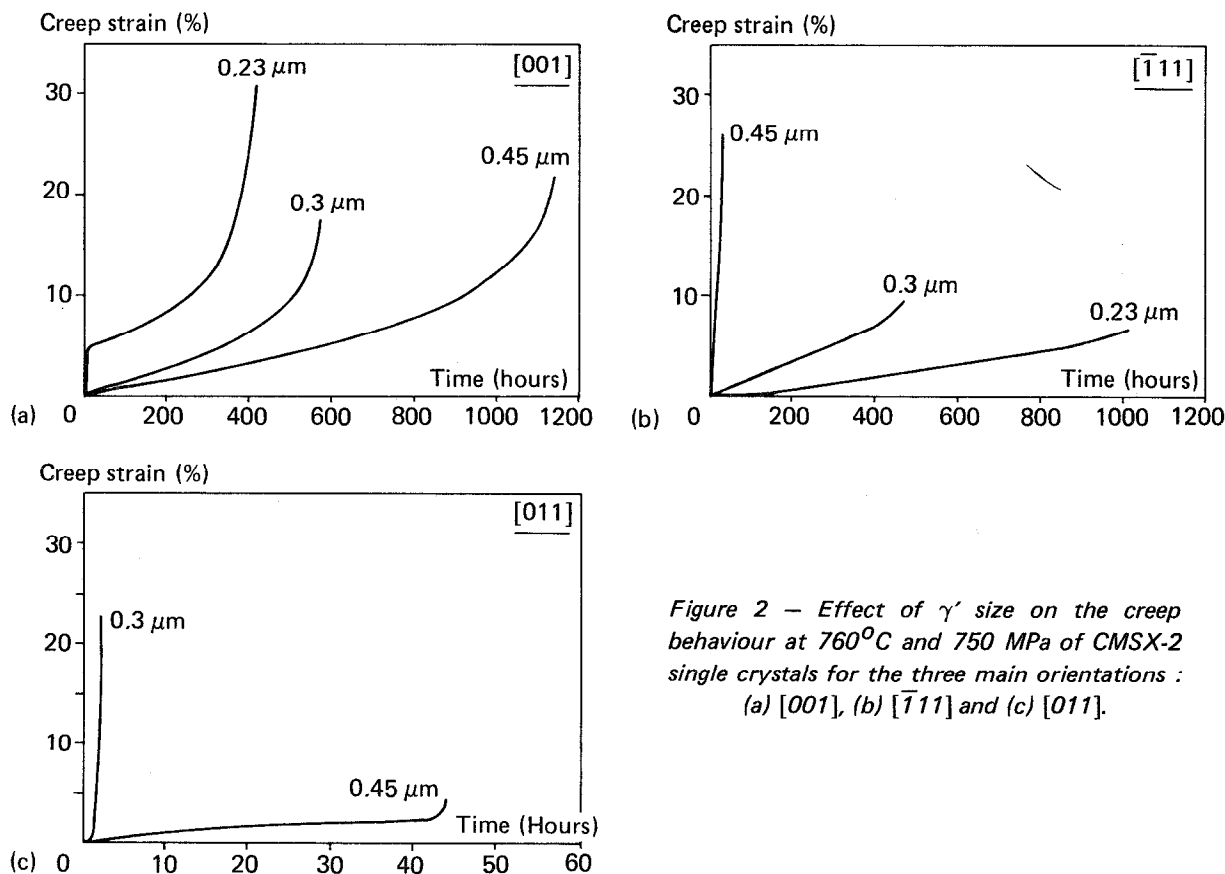


Figure 2 - Effect of  $\gamma'$  size on the creep behaviour at 760°C and 750 MPa of CMSX-2 single crystals for the three main orientations : (a) [001], (b)  $\bar{1}11$  and (c) [011].

The creep tests on alloy 454 were restricted to single crystals containing  $\gamma'$  precipitates of about 0.5  $\mu\text{m}$  in size. As shown in Figure 3 the rupture lives decrease as one moves away from the [001] orientation, but the orientations near  $\bar{1}11$  and [011] show high creep rates and very poor creep strengths. The creep behaviour of this alloy is very similar to that of the CMSX-2 alloy containing 0.45  $\mu\text{m}$   $\gamma'$  particles. It is also worth mentioning that in both these alloys the stress rupture properties do not show any drastic drop up to misorientations of about 15° around [001].

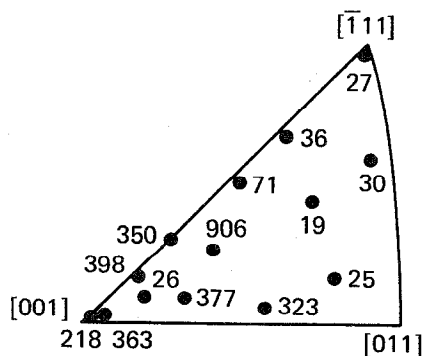


Figure 3 - Effect of orientation on the stress rupture life (in hours) at 760°C and 758 MPa of alloy 454 single crystal ( $\gamma'$  size = 0.5  $\mu\text{m}$ ).

In order to confirm the spectacular effect of the precipitation heat treatment on the creep behaviour of  $\bar{1}11$  oriented crystals, creep tests were run at 760°C and 750 MPa on two other single crystal alloys, MXON and CMSX-4 containing  $\gamma'$  precipitates of two different sizes. Again, in the MXON alloy the highest creep strength along the  $\bar{1}11$  axis was obtained with the finest  $\gamma'$  precipitates. Indeed, for the  $\bar{1}11$  orientation at 760°C and 750 MPa the rupture life of specimens containing 0.2  $\mu\text{m}$  precipitates is over 1800 hours, whereas the life with 0.36  $\mu\text{m}$  precipitates drops to about 50 hours. For the

[001] oriented crystals the decrease in  $\gamma'$  precipitate size from 0.36 to 0.2  $\mu\text{m}$  results in a substantial increase in the primary creep amplitude and a two-fold decrease in creep life as already observed in the CMSX-2 alloy.

The effect of precipitate size on creep is much more subtle in the case of Re-bearing alloy CMSX-4. Typical creep curves for the [001] and  $[\bar{1}11]$  CMSX-4 specimens are shown in Figure 4. Increasing the  $\gamma'$  size from 0.22 to 0.34  $\mu\text{m}$  again leads to a two-fold increase in the creep life along [001], by reducing the primary creep strain amplitude and lowering the secondary creep rate. The effect of  $\gamma'$  size on the creep life of  $[\bar{1}11]$  crystals was however much less pronounced than for CMSX-2 and MXON alloys:  $[\bar{1}11]$  single crystals of CMSX-4 containing precipitates with mean sizes of 0.22 and 0.34  $\mu\text{m}$  showed comparable stress-rupture lives, although their creep behaviours were significantly different. So, by reducing the  $\gamma'$  size from 0.34 to 0.22  $\mu\text{m}$ , the time for 1% creep increased by a factor of ten, and the minimum creep rate was divided by the same factor. Concurrently, the elongation to rupture became ten times smaller, the net result being that the rupture lives were not significantly affected by the  $\gamma'$  particle size. However, when the particle size in this alloy is about 0.5  $\mu\text{m}$ , the creep strength of  $[\bar{1}11]$  crystals is significantly reduced compared to the  $[\bar{1}11]$  crystals containing smaller precipitates, but it remained much higher than those of the  $[\bar{1}11]$  CMSX-2 and MXON crystals containing precipitates of comparable sizes.

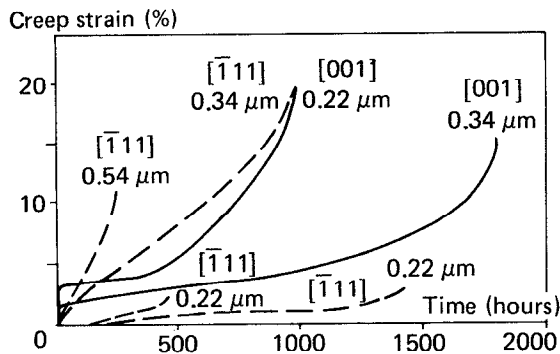


Figure 4 — Effect of  $\gamma'$  size on the creep behaviour at 760°C and 750 MPa of [001] and  $[\bar{1}11]$  CMSX-4 single crystals.

The creep lives at 850°C and 500 MPa of the CMSX-2 and MXON single crystal alloys are still anisotropic, but the effects of orientation and heat treatments are less pronounced than at 760°C. For the CMSX-2 alloy containing 0.3  $\mu\text{m}$  precipitates, the strongest orientation is  $[\bar{1}11]$ , while the [011] oriented crystals exhibited poorest creep lives. Increasing the  $\gamma'$  size to 0.45  $\mu\text{m}$  improved the strength of [001] specimens by a factor of two, whereas the creep life of  $[\bar{1}11]$  crystals was reduced by a factor of five. The creep tests performed on the MXON alloy confirmed the beneficial effect of decreasing the  $\gamma'$  size on the creep lives of  $[\bar{1}11]$  single crystals, as shown in Figure 5. By reducing the precipitate size from 0.36 to 0.2  $\mu\text{m}$ , the creep life of  $[\bar{1}11]$  specimens was improved by a factor of ten, while preserving a high ductility.

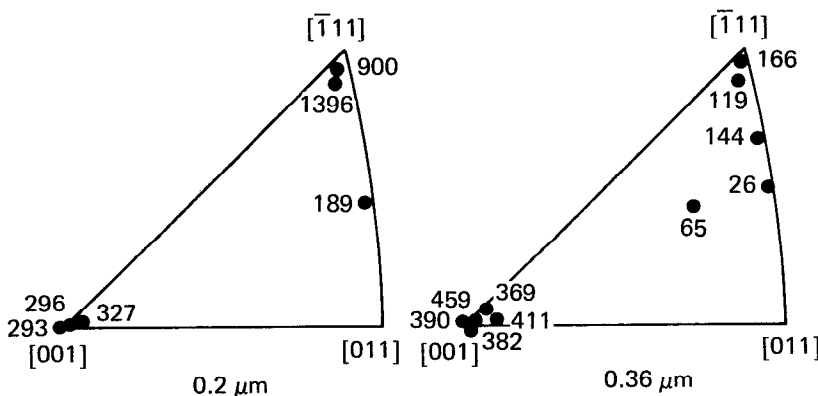


Figure 5 — Effect of orientation and  $\gamma'$  size on the stress rupture life at 850°C and 500 MPa of MXON single crystals.

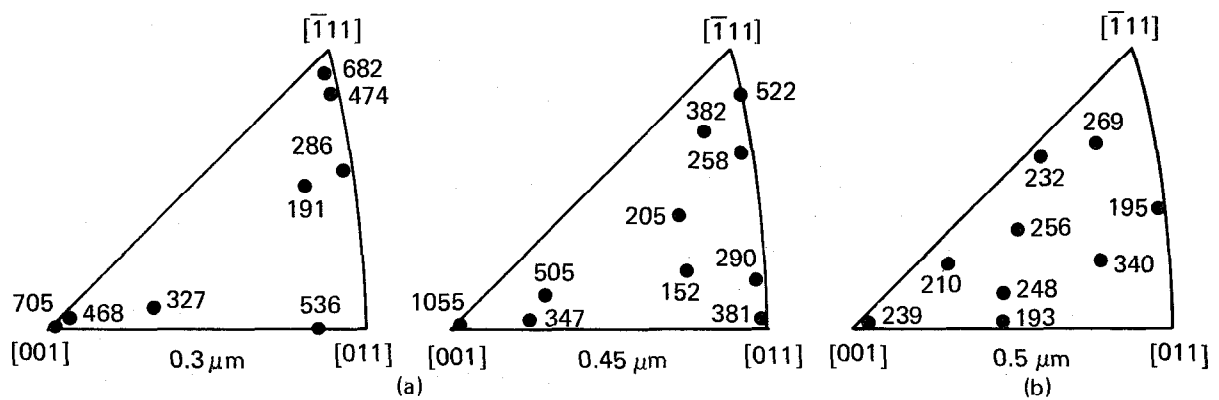


Figure 6 — Effect of orientation and  $\gamma'$  size on the high temperature stress rupture life of single crystals :  
(a) CMSX-2, 1050°C, 120 MPa ; (b) alloy 454, 980°C, 200 MPa.

### Creep properties at high temperature (980-1050°C)

Creep tests were performed at 980°C and 200 MPa on alloy 454 single crystals containing 0.5  $\mu\text{m}$  precipitates and at 1050°C and 120 MPa on CMSX-2 single crystals containing 0.3 and 0.45  $\mu\text{m}$   $\gamma'$  particles. The creep lives are reported in the stereographic triangles of Figure 6.

In this high temperature creep range, the creep life of the alloy 454 did not depend on the crystal orientation. In the case of the CMSX-2 alloy containing the largest precipitates, the highest creep strength is still obtained along [001], while other orientations exhibited creep lives in the range 150-500 hours. For the CMSX-2 alloy containing 0.3  $\mu\text{m}$   $\gamma'$  particles, the highest creep strength was obtained around [001], [111] and [011]. Orientations away from the main directions showed a weaker creep strength. The general creep behaviour at 1050°C of the CMSX-2 single crystal alloy is however much less anisotropic than at lower temperatures.

### Discussion

The typical deformation microstructures generated during primary creep at 760°C and 750 MPa of [001] and [111] oriented CMSX-2 single crystals containing  $\gamma'$  precipitates with sizes in the range 0.22-0.45  $\mu\text{m}$  are shown in Figures 7 and 8. In the [001] single crystals containing the largest precipitates, the deformation operated by homogeneous {111}<110> multiple slip in the matrix (Figure 7a), leading rapidly to the formation of dense dislocation networks at the  $\gamma/\gamma'$  interfaces. Reducing the  $\gamma'$  size to 0.22  $\mu\text{m}$  promoted extensive cooperative shearing of the  $\gamma/\gamma'$  structure by {111}<112> slip (Fig. 7b). The precipitates are sheared by  $1/3$ <112> dislocations with the creation of superlattice intrinsic and extrinsic stacking faults (SISF and SESF). The planar character of this mode of deformation promotes heterogeneous deformation and short rupture lives. The increase in the primary creep strain, the accelerated secondary creep rate and the reduced creep life are clearly related to this transition from the  $\gamma'$  by-passing Orowan mechanism by {111}<110> slip to the  $\gamma/\gamma'$  cooperative shearing mechanism by {111}<112> slip. Whatever the deformation mechanism, more than one slip system is always activated, which agrees with the fact that in the [001] orientation several slip systems are equally stressed, respectively eight for {111}<110> slip (Schmid Factor = 0.41) and four for {111}<112> slip (S.F. = 0.47). Strain hardening due to intersecting slip causes the transition from primary to secondary creep stage. The homogeneous character of deformation by {111}<110> slip favours a rapid strain hardening and the extent of primary creep is rather limited, which improves the overall creep behaviour.

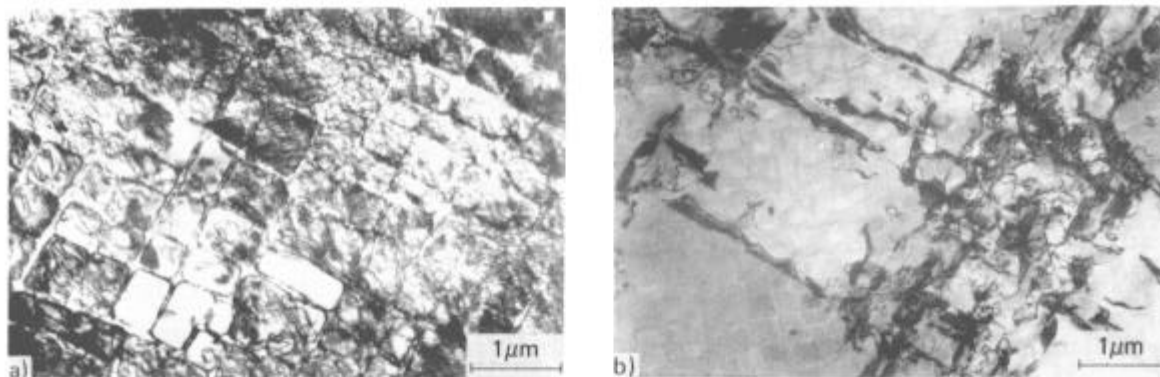


Figure 7 – Dislocation structures during primary creep at 760°C and 750 MPa of [001] CMSX-2 single crystals :  
(a)  $\gamma'$  size = 0.45  $\mu\text{m}$ ,  $\epsilon$  = 0.2 % ; (b)  $\gamma'$  size = 0.23  $\mu\text{m}$ ,  $\epsilon$  = 2 %.

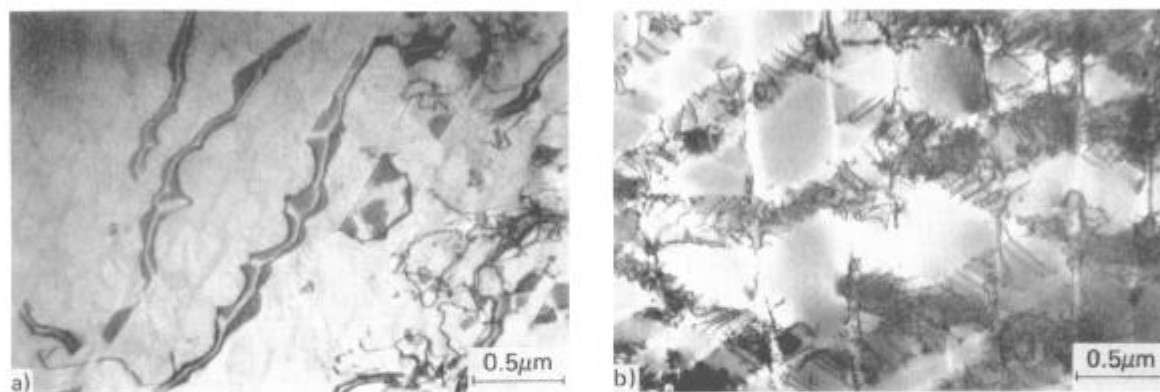


Figure 8 – Dislocation structures during primary creep at 760°C and 750 MPa of  $[\bar{1}11]$  CMSX-2 single crystals :  
(a)  $\gamma'$  size = 0.23  $\mu\text{m}$ ,  $\epsilon$  = 0.6 % ; (b)  $\gamma'$  size = 0.45  $\mu\text{m}$ ,  $\epsilon$  = 1.5 %.

Analysis of the creep deformation microstructures in the [011] CMSX-2 single crystals deformed at 760°C shows that the largest  $\gamma'$  particles favoured homogeneous (111) $[\bar{1}01]$  single slip in the matrix. Moreover, a lot of precipitates are individually sheared by (111) $[\bar{2}11]$  slip with the creation of superlattice stacking faults. When the  $\gamma'$  size is decreased to 0.3  $\mu\text{m}$ , the deformation occurred by (111) $[\bar{2}11]$  extensive planar single slip through the  $\gamma/\gamma'$  structure. In this orientation, the Schmid Factors for these slip systems are the same as for the [001] orientation. Although the [011] orientation favours, theoretically, deformation on two equally stressed slip systems, the rotation of the single crystals induced by the creep deformation tends to move the tensile axis away from [011] and favours single slip. In both cases, the creep life of the single crystals is short due to the absence of strain hardening. The specimens containing the smallest precipitates, however, always showed the highest creep rate due to the operation of extensive heterogeneous (111) $[\bar{2}11]$  slip.

The same heterogeneous deformation mechanism is involved during the primary creep of  $[\bar{1}11]$  CMSX-2 single crystals containing the smallest precipitates (0.23  $\mu\text{m}$ ) (Fig. 8a). The deformation is however limited to the (111) primary slip plane. These specimens showed a better creep strength than the corresponding [001] crystals, which deform by the same creep deformation mechanism. The Schmid Factor for these  $\{111\}\langle 112 \rangle$  slip systems is clearly smaller for  $[\bar{1}11]$  than for [001] (respectively 0.31 and 0.47). The smaller resolved shear stress thus justifies the lower creep rate exhibited by the  $[\bar{1}11]$  oriented single crystals, even if the deformation operates by single slip, as observed during the initial stage of creep. This argument was previously advanced to explain the optimum creep strength of  $[\bar{1}11]$  Mar-M 247 single crystals at 774°C (6). Increasing the precipitate mean size to 0.3  $\mu\text{m}$



promoted Orowan bowing of matrix dislocations between the  $\gamma'$  particles, instead of shearing by  $\{111\}\langle 112 \rangle$  slip, thereby resulting in an increase in the creep rate. During the primary creep, the deformation is inhomogeneous, some areas being free of dislocations, which suggests that there is a strong resistance to deformation by Orowan by-passing. An increase in the  $\gamma'$  size to 0.45  $\mu\text{m}$  decreases the Orowan stress, which leads to a homogeneous deformation structure in the matrix (Fig. 8b). Despite the fact that  $[\bar{1}11]$  is a multiple slip orientation (six equally stressed  $\{111\}\langle 110 \rangle$  slip systems with F.S. = 0.275), careful analysis of the dislocations in near- $[\bar{1}11]$  oriented crept specimens showed that the primary creep deformation operated mainly by coplanar slip in the primary slip plane (111) along the  $[\bar{1}10]$  and  $[101]$  directions (8). This deformation mode causes only a weak strain hardening, which explains the high creep rates observed in this case. The absence of secondary creep stage seems to indicate that the first activated slip system remains predominant throughout the life of the  $[\bar{1}11]$  single crystals. The relatively low value of the Schmid Factor would not allow to activate the conjugate slip systems contrary to the case of  $[001]$  crystals, where multiple slip is operative at the beginning of the primary creep stage. No cube slip was observed for this orientation at 760°C.

T.E.M. analysis performed on MXON, CMSX-4 and alloy 454 single crystals crept at 760°C showed the same overall features as in CMSX-2. For instance, decreasing the  $\gamma'$  size to 0.22  $\mu\text{m}$  in the CMSX-4 alloy promotes heterogeneous deformation by  $\{111\}\langle 112 \rangle$  planar slip instead of homogeneous  $\{111\}\langle 110 \rangle$  slip in the matrix. This creep mechanism transition gave rise to the same effects as in CMSX-2, i.e. increase of the primary creep strain along  $[001]$  and decrease of the secondary creep rate along  $[\bar{1}11]$ . In the case of  $[\bar{1}11]$  CMSX-4 single crystals with the finest precipitates, the fracture surface was planar and parallel to (111). The low elongation to rupture which resulted in a short rupture life was therefore due to the planar nature of deformation. On the other hand, the alloy 454 single crystals containing precipitates with a mean size of 0.5  $\mu\text{m}$  deformed mainly by  $\{111\}\langle 110 \rangle$  slip in the matrix, which is in accordance with the good creep behaviour of the  $[001]$  specimens and the very poor creep strength along  $[\bar{1}11]$ , as explained in the case of the CMSX-2 crystals containing the largest precipitates.

The dislocation structures observed after creep at 850°C and 500 MPa in the CMSX-2, CMSX-4 and MXON  $[001]$  single crystals are homogeneous independently of the size of the precipitates. The deformation operated mainly in the  $\gamma$  matrix by  $\{111\}\langle 110 \rangle$  slip. Moreover, some  $\gamma'$  particles were shown to be individually sheared by  $\{111\}\langle 112 \rangle$  slip or by pairs of  $\frac{1}{2}\langle 110 \rangle$  dislocations. Extensive shearing of the  $\gamma/\gamma'$  structure by  $\{111\}\langle 112 \rangle$  slip was never observed at 850°C and 500 MPa, which explains the limited amplitude of the primary creep strain even in the case of  $[001]$  crystals containing the smallest precipitates. The better creep strength of the  $[\bar{1}11]$  CMSX-2 and MXON single crystals containing the finest precipitates, compared to the corresponding  $[001]$  oriented specimens, may be explained by the reduced value of the Schmid Factor for  $\{111\}\langle 110 \rangle$  slip, i.e. 0.275 vs. 0.41. Again, the  $[011]$  orientation is weak due to operation of single slip. The improvement of the creep strength of the  $[001]$  CMSX-2 single crystals as the precipitate size increases from 0.3 to 0.45  $\mu\text{m}$  has been shown previously to be related to the reduction of the kinetics of dislocation climb during the secondary creep stage.<sup>(11)</sup> In the case of  $[\bar{1}11]$ , the reduction of the creep strength when the  $\gamma'$  size increases can be interpreted using arguments similar to those advanced to explain the creep behaviour at 760°C. However, the major difference at 850°C, compared with 760°C, is that the deformation occurs in the matrix by  $\{111\}\langle 110 \rangle$  slip, even in the case of the finest precipitates.

The main feature observed during the high temperature creep of nickel-based superalloys is the rapid coarsening of the strengthening  $\gamma'$  particles.

Several studies have shown that, in [001] single crystal superalloys where the  $\gamma/\gamma'$  misfit is negative at the testing temperature,  $\gamma'$  rafts develop normal to the tensile axis. The low creep rates and long rupture lives observed in these cases are generally thought to be due to this particular morphology of the  $\gamma'$  phase, which inhibits dislocation climb around them. Such  $\gamma'$  rafts normal to the [001] stress axis have previously been observed in CMSX-2 (9), CMSX-4 (2) and MXON (4) single crystals during creep at high temperature. Additional observations made on a  $[\bar{1}11]$  oriented CMSX-2 single crystal crept at 1050°C show that the precipitates apparently coarsen parallel to the three {001} planes, which results in irregular shaped coarse  $\gamma'$  particles. In view of the fact that, in general, the creep strengths are not strongly dependent on orientation one may question the so-called beneficial role played by the rafted  $\gamma'$  morphology for [001] oriented specimens at high temperature. Certainly, careful further work is required to elucidate this problem.

### Conclusions

This investigation shows some spectacular effects of the crystal orientation and heat treatments on the creep behaviour and strength of a number of single crystal superalloys. The salient features can be summed up as follows:

1. At intermediate temperatures (760-850°C), the creep behaviour of nickel-base single crystal superalloys is extremely sensitive to the orientation and  $\gamma'$  precipitate size. For a  $\gamma'$  size in the range 0.35-0.5  $\mu\text{m}$ , the highest creep strength is obtained near [001], whereas orientations near the  $[\bar{1}11]$ -[011] boundary of the standard stereographic triangle exhibit very short creep lives. When the  $\gamma'$  size decreases to 0.2  $\mu\text{m}$ , the longest creep lives are exhibited, in decreasing order, by the crystals oriented near  $[\bar{1}11]$ , [001] and [110]. The anisotropy in creep between the [001] and  $[\bar{1}11]$  orientations can therefore be reduced by appropriate precipitation heat treatments. The creep strengths, however, remain extremely poor near the [011] orientation.
2. At high temperatures (980-1050°C), the creep behaviour of the single crystal superalloys is much less sensitive to orientation and  $\gamma'$  size than at intermediate temperatures. The [001] oriented single crystals develop a rafted  $\gamma'$  structure normal to the tensile stress axis, while the  $\gamma'$  precipitates coarsen rather irregularly in the  $[\bar{1}11]$  specimens.

### References

1. K. Harris, G.L. Erickson, and R.E. Schwer, "CMSX Single Crystal, CM DS & Integral Wheels, Properties and Performance", High Temperature Alloys for Gas Turbines and Other Applications 1986, ed. W. Betz & al. (Dordrecht, Holland: D. Reidel Publishing Company, 1986), 709-728.
2. K. Harris, G.L. Erickson, and R.E. Schwer, "Development of an Ultra High Strength Single Crystal Superalloy CMSX-4 for Small Gas Turbines" (Paper presented at the 1983 TMS-AIME Fall Meeting, Philadelphia, Pennsylvania, 3 October 1983).
3. M. Gell, D.N. Duhl, and A.F. Giamei, "The Development of Single Crystal Superalloy Turbine Blades", Proc. of the Fourth International Symposium on Superalloys, ed. J.K. Tien & al. (Metals Park, OH: ASM, 1980), 205-214.

4. T. Khan, P. Caron, and C. Duret, "The Development and Characterization of a High Performance Experimental Single Crystal Superalloy", Proc. of the Fifth International Symposium on Superalloys, ed. M. Gell, C.S. Kortovich, R.H. Bricknell, W.B. Kent, and J.F. Radavich (Warrendale, PA: The Metallurgical Society of AIME, 1984), 145-155.
5. B.H. Kear, and B.J. Piearcey, "Tensile and Creep Properties of Single Crystals of the Nickel-Base Superalloy Mar-M200", Trans. TMS-AIME, 239 (1967) 1209-1215.
6. R.A. MacKay, and R.D. Maier, "The Influence of Orientation on the Stress Rupture Properties of Nickel-Base Superalloy Single Crystals", Met. Trans. A, 13A (1982) 1747-1754.
7. M.R. Winstone, "The Effect of Orientation on the Properties of Single Crystals of the Nickel Superalloy Mar-002" (NGTE Memorandum M81017, 1981).
8. P. Caron, T. Khan, and Y.G. Nakagawa, "Effect of Orientation on the Intermediate Temperature Creep Behaviour of Ni-Base Single Crystal Superalloys", Scripta Met., 20 (1986) 499.
9. P. Caron, and T. Khan, "Improvement of Creep Strength in a Nickel-Base Single Crystal Superalloy by Heat Treatment", Mat. Sci. and Eng., 61 (1983) 173-184.
10. T. Khan, P. Caron, D. Fournier, and K. Harris, "Single Crystal Superalloys for Turbine Blades", Matériaux et Techniques, 10-11 (1985) 567-578.
11. P. Caron, P.J. Henderson, T. Khan, and M. McLean, "On the Effects of Heat Treatments on the Creep Behaviour of a Single Crystal Superalloy", Scripta Met., 20 (1986) 875-880.